



HAL
open science

Kinetic Analysis of the Immortal Ring-Opening Polymerization of Cyclic Esters: A Case Study with Tin(II) Catalysts

Lingfang Wang, Valentin Poirier, Fabio Ghiotto, Manfred Bochmann, Roderick D. Cannon, Jean-François Carpentier, Yann Sarazin

► **To cite this version:**

Lingfang Wang, Valentin Poirier, Fabio Ghiotto, Manfred Bochmann, Roderick D. Cannon, et al.. Kinetic Analysis of the Immortal Ring-Opening Polymerization of Cyclic Esters: A Case Study with Tin(II) Catalysts. *Biomacromolecules*, 2014, 47 (8), pp.2574-2584. 10.1021/ma500124k . hal-01114346

HAL Id: hal-01114346

<https://univ-rennes.hal.science/hal-01114346>

Submitted on 15 Dec 2021

HAL is a multi-disciplinary open access archive for the deposit and dissemination of scientific research documents, whether they are published or not. The documents may come from teaching and research institutions in France or abroad, or from public or private research centers.

L'archive ouverte pluridisciplinaire **HAL**, est destinée au dépôt et à la diffusion de documents scientifiques de niveau recherche, publiés ou non, émanant des établissements d'enseignement et de recherche français ou étrangers, des laboratoires publics ou privés.

Kinetic Analysis of the Immortal Ring-Opening Polymerization of Cyclic Esters: A Case Study with Tin(II) Catalysts

Lingfang Wang,[†] Valentin Poirier,[†] Fabio Ghiotto,[‡] Manfred Bochmann,^{*,‡}

Roderick D. Cannon,^{*,‡} Jean-François Carpentier^{*,†} and Yann Sarazin^{*,†}

Email addresses: m.bochmann@uea.ac.uk; r.cannon@uea.ac.uk; jean-francois.carpentier@univ-rennes1.fr; yann.sarazin@univ-rennes1.fr

[†] *Organometallics: Materials and Catalysis, Institut des Sciences Chimiques de Rennes, UMR 6226 CNRS – Université de Rennes 1, Campus de Beaulieu, 35042 Rennes Cedex, France.*

[‡] *Wolfson Materials and Catalysis Centre, School of Chemistry, University of East Anglia, Norwich NR4 7TJ, UK.*

Abstract

A kinetic analysis of the metal-catalyzed immortal ring-opening polymerization (ROP) of cyclic esters is presented, based on a first-principles approach without making assumptions regarding the active species. The kinetics of all immortal ROP reactions performed with a metal catalyst and an exogenous chain transfer agent are characterized by the initiation, propagation and exchange rate constants (k_i , k_p and k_e , respectively). Curve fitting to this kinetic scheme in the initial stage of the polymerization allows the extraction of k_i and k_p from a single experiment. This has been illustrated for the ROP of L-lactide using tin(II) complexes of the type $\{LO^i\}Sn(X)$ ($\{LO^i\}$ = aminophenolate ancillary ligand, $X = N(SiMe_3)_2$ or methyl (*S,S*)-lactate), $Sn(OiPr)_2$ or $Sn(N(SiMe_3)_2)_2$ as precatalysts paired with excess *i*PrOH as a co-activator. Non-linear regressions ($R^2 > 0.999$)

illustrate the three possible scenarios, $k_i < k_p$, $k_i = k_p$ and $k_i > k_p$. The kinetic model can be extended to *any* metal (pre)catalyst for the immortal ROP of *any* cyclic ester, as exemplified using trimethylene carbonate as a monomer or employing a germylene precatalyst. A kinetic treatment for the late phase of immortal ROP reactions is introduced, which also gives direct access to k_p . In agreement with the ROP kinetic data for $\{LO^i\}Sn(N(SiMe_3)_2)$, $Sn(OiPr)_2$, $Sn(N(SiMe_3)_2)_2$ and the new $Sn(OiPr)(N(SiMe_3)_2)$ recorded in the presence of various quantities of *i*PrOH, synthetic and $^{119}Sn\{^1H\}$ NMR data provide evidence for reversible production of tin(II) *bis*(alkoxide) when a small excess (1–3 equiv) of alcohol is used with tin(II) precatalysts. It is also shown that, regardless of the identity of the precatalyst, $Sn(OiPr)_2$ and $Sn(O\text{--}polymeryl)_2$ are, respectively, the actual initiating and propagating species when immortal ROP reactions are performed in the presence of a larger excess of alcohol (7 equiv or more *vs.* Sn).

Introduction

The ring-opening polymerization (ROP) of lactide, ϵ -caprolactone, β -butyrolactone or trimethylene carbonate continues to receive growing interest because some of these cyclic esters are derived from biomass and the resulting biocompatible materials offer an attractive range of physical properties.¹ The number of key studies² and review articles³ covering the design of metal catalysts enabling controlled, and often living, ROP reactions is a testimony to the health of the field. The step from academic laboratory to industrial plants is now a key item on the agenda. In this aim, so-called “*immortal*” ROP processes, known since the 1980’s for oxiranes,⁴ offer real promise. Unlike regular *living* polymerizations where each metal centre produces only one polymer chain during the entire process, the use of an inexpensive chain transfer agent (typically an alcohol) in *immortal* polymerizations⁵ allows the production of many macromolecules per catalyst through reversible chain transfer between growing and dormant polymer chains.^{3d,6} The advantages of such reactions have attracted attention,⁷ and efforts are being made to implement them under industrial

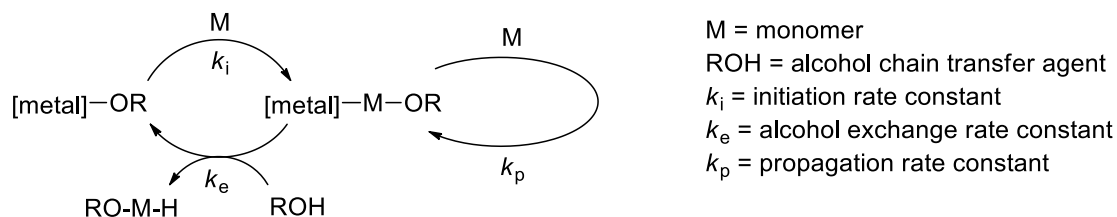
conditions.⁸ Yet, the mechanisms of these reactions, and in particular the kinetic aspects, remain rather obscure.

In spite of all the achievements in terms of catalyst development, industrial processes still rely on tin(II) species such as $\text{Sn}^{\text{II}}(\text{2-ethyl-hexanoate})_2$.^{1,9} Several structurally well-defined tin(II) complexes generally featuring good performance in the polymerization of cyclic esters have also been released.^{2k,10} We have used amino(ether)-phenolate tin(II) complexes to probe some of the mechanistic features of ROP reactions by $^{119}\text{Sn}\{^1\text{H}\}$ NMR spectroscopy and DFT computations,¹¹ and this has led to a kinetic analysis of the (conventional) *living* polymerization of lactide.¹²

Living and immortal polymerizations represent two distinctly different mechanistic scenarios and kinetic regimes: in living ROP the polymer M_n is given by the monomer/initiator ratio, while in immortal ROP it is defined by the monomer/ROH ratio. Duda and Penczek studied in detail the influence of alcohol concentration on the rate of ROP reactions catalyzed by $\text{Sn}(\text{2-ethyl-hexanoate})_2$ and related catalyst precursors, and they were able to detect several trends and identify some active species.⁹ However, a comprehensive kinetic model has to our knowledge not been proposed for immortal polymerizations, and the simple models developed for living ROP cannot be applied to immortal systems. Tolman and Hillmyer assumed a Michaelis-Menten-type kinetic model, based on a pre-formed $\{\text{L}\}\text{AlO}i\text{Pr}$ catalyst in the absence of added alcohol,¹³ and our own previous non-steady-state approach to living ROP also does not take excess alcohol into consideration.¹² The description of immortal systems therefore remains mostly empirical, and kinetic analysis is confined to the determination of partial orders in monomer, (pre)catalyst and transfer agent.^{2r,7,11a} Yet, metallocene-catalyzed olefin polymerization has taught us the virtues of a thorough understanding of the intricacies of polymerization kinetics.¹⁴

We present here a general kinetic mechanism of the immortal polymerization of cyclic esters. Our initial attempts to identify Michaelis-Menten-type kinetic behavior in such systems were not successful, and we have therefore developed a model based simply on the known reaction steps in immortal ROP. This kinetic analysis is built on first principles only and makes no *a priori*

assumptions as to the nature of the active species. In addition to the initiation (k_i) and propagation (k_p) parameters that characterize all polymerization reactions, the equations presented here take into account the *exchange* process (chain transfer, k_e) specific to immortal ROP reactions.



The validity of the formal kinetics is then illustrated by a range of experimental data obtained during the polymerization of L-lactide or trimethylene carbonate mediated by group 14 complex / *i*PrOH binary catalysts, since these catalysts lend themselves well to kinetic monitoring (Chart 1). It is shown that non-linear regression of a *single* kinetic experiment allows the rapid and accurate determination of k_i and k_p . The influence of the ROH/Sn molar ratio with respect to the nature of the active species in these catalyst systems is discussed in the light of $^{119}\text{Sn}\{^1\text{H}\}$ NMR spectroscopic and kinetic investigations.

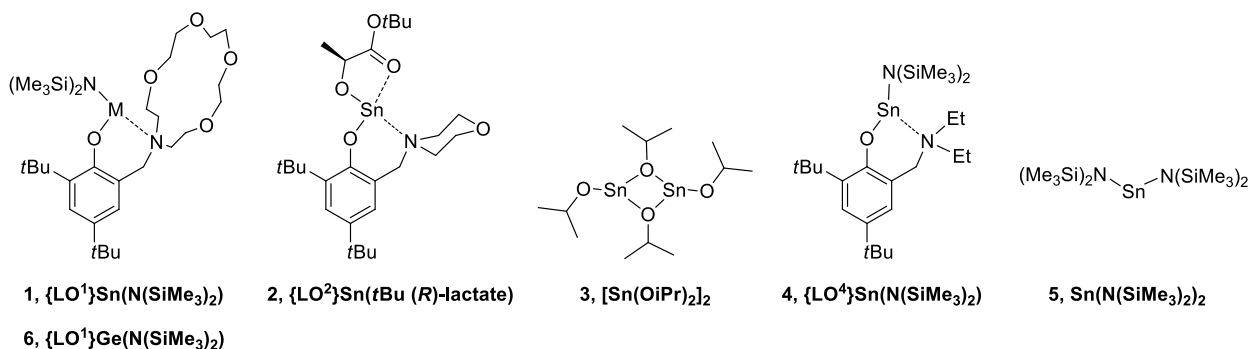


Chart 1.

Results and Discussion

1. Kinetic analysis of *immortal* polymerizations: $[\text{ROH}] \gg [\text{catalyst}]$.

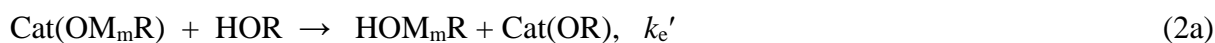
So-called “immortal” ring-opening polymerizations of cyclic esters are performed in the presence of an alcohol ROH (such as isopropanol). Ring-opening and protolytic exchange reactions produce OH-terminated macromonomers $\text{R}-(\text{M})_n\text{-OH}$, with $[\text{OH}]$ remaining constant throughout the

whole process. Initially the catalyst Cat carries OR function, denoted as Cat(OR). For our kinetic mechanism we define catalyst initiation as the first insertion of monomer M into a metal–alkoxide bond, characterized by the rate constant k_i ; this process converts C(OR) into C(OMR). Subsequent insertion steps are taken to proceed with the propagation rate k_p . For simplicity it is assumed that k_p is identical for all subsequent chain growth steps. These steps are summarised in eq 1(a)-(c).

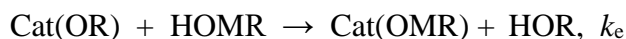


etc.

Since in an immortal polymerization an excess of ROH is present that interchanges with the growing polymer chain, in principle this exchange also has to be considered, eq 2(a) and 2(b). As long as unconsumed alcohol ROH is present, the exchange will proceed with the rate k_e' , which may differ from the rate k_e once all ROH is consumed.



1.1 Interchange with no depletion of monomer. As shown above, the immortal ROP consumes the added alcohol ROH in the initial phase. However, since the exchange reactions are reversible, as long as some Cat(OR) remains, ROH may also be regenerated:



The approximation $k_e' = k_e$ was considered a reasonable working hypothesis and was applied to maintain the scheme mathematically manageable.¹⁵ Note that provided k_e is sufficiently large, the

exact value of the exchange rate constants do not impact the overall kinetics (*vide infra*). It can be shown (for full derivation of the kinetic model, see Supporting Information) that:

$$[\text{Cat(OR)}] = \frac{(k_e [\text{Cat}]_T + \lambda_1)\lambda_2 e^{\lambda_1 t} - (k_e [\text{Cat}]_T + \lambda_2)\lambda_1 e^{\lambda_2 t}}{k_e (\lambda_2 - \lambda_1)} \quad (3a)$$

$$[\text{ROH}] = \frac{(\lambda_2 e^{\lambda_1 t} - \lambda_1 e^{\lambda_2 t})}{\lambda_2 - \lambda_1} [\text{OH}]_T \quad (3b)$$

where λ_1 and λ_2 are given by

$$\lambda_{1,2} = \frac{1}{2} \{ -(k_e [\text{OH}]_T + k_i [\text{M}] + k_e [\text{Cat}]_T) \pm [(k_e [\text{OH}]_T + k_i [\text{M}] + k_e [\text{Cat}]_T)^2 - 4 k_i [\text{M}] k_e [\text{Cat}]_T]^{1/2} \} \quad (3c)$$

1.2 The Monomer Conversion. In immortal ROP the enchaind monomers M are distributed over OH-terminated (major) and C-terminated (minor) molecules. The conversion, *i.e.* the concentration of bound monomer $[\text{M}]_B$, is given by:

$$[\text{M}]_B = k_p [\text{M}] [\text{Cat}]_T t + (k_i - k_p) k_e^{-1} [\text{M}] (\lambda_2 - \lambda_1)^{-1} \times \{ (k_e [\text{Cat}]_T + \lambda_1) \lambda_1^{-1} \lambda_2 [-1 + e^{\lambda_1 t}] - (k_e [\text{Cat}]_T + \lambda_2) \lambda_1 \lambda_2^{-1} [-1 + e^{\lambda_2 t}] \} \quad (4)$$

with $\lambda_{1,2}$ as defined in eq (3c). Eq (4) (cf. Supporting Information) describes the rate of monomer consumption as a function of time. Since for a given experiment $[\text{Cat}]_T$, $[\text{HO}]_T$ and $[\text{M}]$ are known experimental values, this equation can be fitted to experimental curves using the three rate constants k_e , k_i and k_p which characterize all immortal ROP reactions. The initiation phase, whether under “immortal” or “living” conditions, is often overlooked in available kinetic analyzes of ROP reactions but can provide an explanation for the positive or negative curvature of the consumption profiles in the early stages of the reaction.

2. Tin-catalyzed immortal ring-opening polymerizations

Tin(II) precatalysts are suited to the monitoring of ROP reactions by NMR techniques,^{11,12} because they offer a good compromise of activity, control over the polymerization parameters and robustness.¹⁶ The applicability of eq (4) was therefore tested using the tin(II) catalyst shown in Chart 1.

A range of polymerizations carried out in toluene-*d*₈ at 25–80 °C were monitored by ¹H NMR spectroscopy. The immortal ROP of L-LA mediated by the binary group 14 precatalysts **1–6** activated by a molar excess of *i*PrOH shows an initiation phase, as well as the effect of monomer depletion when conversion exceeds 60%. The initiation phase is more evident when plotting the slope of the conversion curve as a function of conversion (Figure 1).

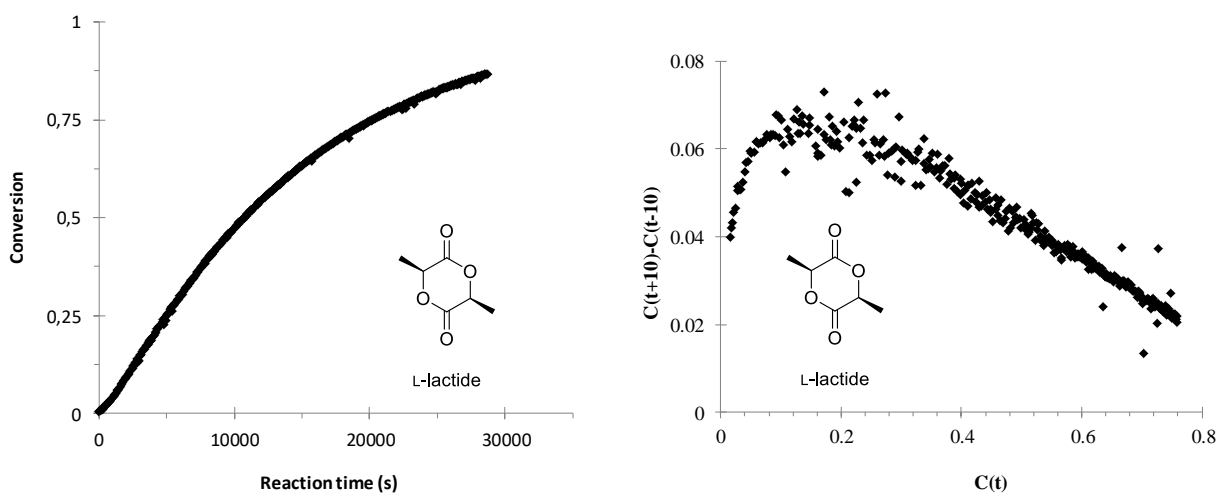


Figure 1. L-LA polymerization catalyzed by **1**/*i*PrOH in toluene, 25 °C. $[\text{Sn}]_{\text{T}} = 5.0 \text{ mM}$, $[\text{L-LA}]_{\text{T}} = 0.33 \text{ M}$, $[\text{L-LA}]_{\text{T}}/[\text{Sn}]_{\text{T}}/[\text{iPrOH}]_{\text{T}} = 66:1:5$. Left: Monomer conversion vs. reaction time. Right: Plot of the slope of conversion curve vs. conversion $C(t)$, showing the initiation phase.

The immortal ROP of L-LA (100 equiv) at 60 °C catalyzed by a mixture of **1** with 10 *i*PrOH ($[\text{L-LA}]_{\text{T}}/[\text{Sn}]_{\text{T}}/[\text{iPrOH}]_{\text{T}} = 100:1:10$; $[\text{L-LA}]_{\text{T}} = 1.0 \text{ M}$) constituted our benchmark experiment: typically for this and all related catalysts, the rate of monomer consumption follows first-order dependence upon monomer concentration. Eyring analysis of data for the ROP of L-LA in the temperature range 40–80 °C gave activation parameters ($\Delta H^{\ddagger} = 13.2 \text{ kcal}\cdot\text{mol}^{-1}$ and $\Delta S^{\ddagger} = -32.8$

cal·K⁻¹·mol⁻¹) comparable with those reported before for related systems;¹⁰ the largely negative value of ΔS^\ddagger points at an associated transition state (cf. Supporting Information Figure S1).

Table 1 collects the observed rate constants (k_{obs}) for Sn(II) catalyzed polymerization reactions performed in toluene-*d*₈ with a large excess of alcohol as a chain transfer agent (5 – 40 equiv *vs.* Sn). The values of k_{obs} are comparable for polymerizations carried out with different precatalysts, all other conditions remaining identical: compare for instance entries 2 and 3, 4 and 5, 6 and 7 or 10 and 11. Comparison of their respective k_{obs} show that the *bis*(amido) precatalyst **5** induces slightly better activity than the heteroleptic amido catalyst precursor **1**.

Non-linear regression was performed to assess the validity of eq (4), substituting [Cat]_T by [Sn]_T for the concentration of the total of tin species involved. The value of k_e for all curve-fitting experiments collected in Table 1 was set to 100 L·mol⁻¹·s⁻¹.¹⁷ The decision to constrain k_e to a high value (*i.e.* $k_e \gg k_i, k_p$) is justified by the fact that well-controlled *immortal* ROP processes produce polymers with narrow molecular weight distributions (typically $M_w/M_n < 1.10$),^{7,11,12} a fact which can only be accounted for by assuming that the rate of exchange between dormant and growing macromolecules is much greater than initiation and chain growth.¹⁸

The values of k_i and k_p determined using eq (4) for *immortal* ROP reactions fall characteristically in the range $0.50 - 5.00 \times 10^{-2}$ L·mol⁻¹·s⁻¹, and are similar to those determined for regular *living* polymerizations catalyzed by the same tin(II) precatalysts under comparable conditions.¹² Since these binary systems exhibit first order kinetics in [monomer] and a zero order dependence in [*i*PrOH] when sufficient excess of alcohol is used (*ca.* 5 – 7 equiv *vs.* the metal, see below), the relationship $k_{\text{obs}} = k_p \times [\text{Sn}]_T$ is verified to an excellent level of accuracy (Table 1).

Table 1. Kinetic parameters for the immortal ROP of L-LA and TMC catalyzed by tin(II)/*i*PrOH binary catalysts.^a

Entry	Sn	M	T (°C)	[M]/[Sn] _T /[<i>i</i> PrOH] _T	[M] (M)	[Sn] _T (mM)	[<i>i</i> PrOH] _T (mM)	$k_{\text{obs}} \times 10^4$ ^b (s ⁻¹)	$k_p \times 10^2$ ^c (L·mol ⁻¹ ·s ⁻¹)	$k_i \times 10^2$ ^c (L·mol ⁻¹ ·s ⁻¹)	$k_p \times 10^2$ ^d (L·mol ⁻¹ ·s ⁻¹)
1	1	L-LA	25	66:1:5	0.33	5.00	25.0	0.72	1.54 ± 0.04	0.62 ± 0.01	1.34 ± 0.002
2	1	L-LA	25	66:1:10	0.33	5.00	50.0	0.92	1.62 ± 0.02	1.00 ± 0.01	1.71 ± 0.002
3	5	L-LA	25	66:1:10	0.33	5.00	50.0	1.06	1.78 ± 0.02	1.81 ± 0.01	2.14 ± 0.001
4	1	L-LA	45	100:1:10	0.50	5.00	50.0	4.72	6.68 ± 0.05	7.36 ± 0.08	8.98 ± 0.03
5	5	L-LA	45	100:1:10	0.50	5.00	50.0	7.21	10.11 ± 0.10	17.37 ± 0.39	14.05 ± 0.01
6	1	L-LA	45	200:1:20	0.50	2.50	50.0	3.02	8.71 ± 0.08	8.82 ± 0.10	11.46 ± 0.03
7	5	L-LA	45	200:1:20	0.50	2.50	50.0	4.34	12.77 ± 0.12	16.51 ± 0.25	17.20 ± 0.01
8	1	L-LA	60	100:1:10	0.50	5.00	50.0	12.46	18.94 ± 0.20	19.50 ± 0.40	25.86 ± 0.05
9	5	L-LA	60	100:1:10	0.50	5.00	50.0	19.13	25.44 ± 0.24	34.49 ± 0.86	37.51 ± 0.20
10	1	L-LA	60	200:1:20	0.50	2.50	50.0	8.30	25.77 ± 0.25	25.86 ± 0.43	33.36 ± 0.05
11	5	L-LA	60	200:1:20	0.50	2.50	50.0	11.65	36.24 ± 0.43	41.45 ± 0.96	48.00 ± 0.10
12	2	L-LA	60	400:1:40	1.00	2.50	100	7.89	22.32 ± 0.21	35.02 ± 1.00	32.33 ± 0.11
13	2	L-LA	60	900:1:90	1.00	1.12	100	4.63	28.90 ± 0.19	30.65 ± 0.48	38.06 ± 0.05
14	1	TMC	60	100:1:10	1.00	10.0	100	2.78	3.05 ± 0.06	1.70 ± 0.04	2.95 ± 0.01
15	1	TMC	60	100:1:16	1.00	10.0	160	2.37	2.65 ± 0.07	1.49 ± 0.03	2.60 ± 0.01
16	1	TMC	60	166:1:16	1.00	6.00	100	1.88	3.35 ± 0.09	1.43 ± 0.04	3.00 ± 0.005

^a Polymerizations in toluene-*d*₈; see experimental section for details. ^b Observed rate constant determined from the semi-logarithmic plot of monomer conversion vs. time. ^c Determined by curve-fitting using eq (4), and arbitrarily setting the value of k_e to 100 L·mol⁻¹·s⁻¹ for all entries. ^d Determined from eq (5) corresponding to the monomer depletion phase.

The validity of our analysis was further supported by comparing values of k_p determined using eq (4) and those obtained by conventional methods for the controlled polymerization of L-LA promoted **2** without added alcohol (*i.e.* under *living* conditions; see below for the role of excess alcohol in *immortal* polymerizations catalyzed by **1–5**/*i*PrOH). The linear plot of k_{obs} vs. $[\text{Sn}]_T$ indicates first order dependence in precatalyst concentration (cf Supporting Information, Figure S2), and the propagation rate constant obtained as the slope ($k_p = 4.84 \pm 0.01 \times 10^{-2} \text{ L}\cdot\text{mol}^{-1}\cdot\text{s}^{-1}$) was commensurate with those determined by fitting the same data sets to eq (4) with $[i\text{PrOH}]_0 = 0 \text{ mol}\cdot\text{L}^{-1}$ (in the range $4.09 \pm 0.06 - 4.83 \pm 0.01 \times 10^{-2} \text{ L}\cdot\text{mol}^{-1}\cdot\text{s}^{-1}$).¹⁹ Conventional analysis (*i.e.* plots of $\ln(k_{\text{obs}})$ vs. $\ln([\text{Sn}]_T)$) affords of course a single value of k_p , with no access to k_i , for a complete set of experiments where $[\text{Sn}]_T$ is changed, while curve-fitting each of these experiments to the kinetic model affords its own value of k_p .

Cases where an initiation period is observed are characterized by $k_i < k_p$ (entries 1 – 2 and 14 – 16). In the present tin system the two rate constants remain roughly of the same order of magnitude. As expected from the kinetic mechanism, there is no impact on the molecular weight distributions of the polymers that are produced with these tin(II) catalyts: independent of the reactions conditions, $M_w/M_n < 1.11$ is systematically found at partial monomer conversion (cf. SI Table S2).

An example of immortal ROP of L-LA catalyzed by the **1**/*i*PrOH binary catalyst submitted to curve-fitting with eq (4) is presented in Figure 2. The curve fitting for enchainment monomer $[\text{M}]_B$ as function of reaction time depicted shows that at 25 °C, initiation of the polymerization of $\text{M} = \text{L-LA}$ catalyzed by **1** + 5 *i*PrOH is slower than propagation, $k_i = 0.62 \pm 0.01 \times 10^{-2}$ and $k_p = 1.54 \pm 0.04 \times 10^{-2} \text{ L}\cdot\text{mol}^{-1}\cdot\text{s}^{-1}$; the curve shape is typical of such scenarios.

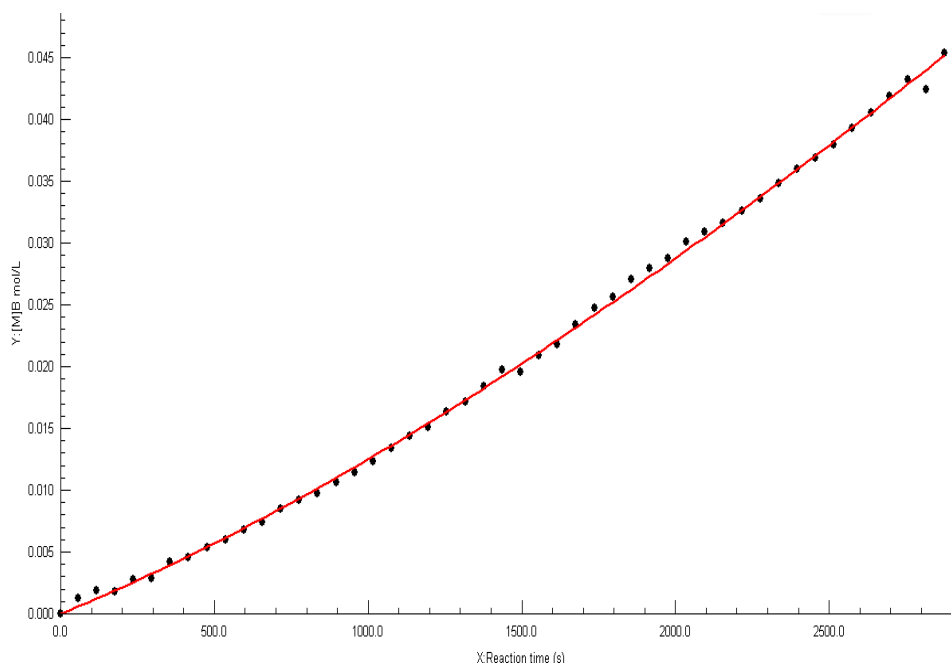


Figure 2. Curve fitting for enchainment monomer $[L-LA]_B$ vs. time ($[L-LA]_{B,maximum} = 0.33$ M) for the immortal ROP of L-LA catalyzed by the Sn(II) amide precatalyst **1** and *i*PrOH. Reaction conditions: solvent = toluene-*d*₈, 25 °C, $[L-LA]_T/[Sn]_T/[iPrOH]_T = 66:1:5$, $[Sn]_T = 5.0$ mM, $[L-LA]_T = 0.33$ M. Fitted curve: plain line; experimental data: black dots; $k_i = 0.62 \pm 0.01 \times 10^{-2} \text{ L}\cdot\text{mol}^{-1}\cdot\text{s}^{-1}$, $k_p = 1.54 \pm 0.04 \times 10^{-2} \text{ L}\cdot\text{mol}^{-1}\cdot\text{s}^{-1}$; $R^2 > 0.999$.

For representative curve-fitting plots of $[M]_B$ vs. time for other experiments in Table 1 see Supporting Information (Figures S3 – S8). In all cases, the agreement between the theoretical curves established from eq (4) and the experimental data was excellent ($R^2 \approx 0.999$). Examples where the initiation is *faster* than propagation were obtained for more reactive systems and/or higher temperature.²⁰ The polymerization of L-LA catalyzed by the homoleptic **5** + 10 *i*PrOH at 45 °C (Table 1, entry 5; SI Figure S9) and that catalyzed by the tin(II) lactate **2** + *i*PrOH at 60 °C with high loadings of monomer and chain transfer agent (Table 1, entry 12; SI Figure S10) are representative examples.

Trimethylenecarbonate. TMC shows similar behavior, but with a more pronounced initiation phase (Figure 3). The immortal ROP of TMC mediated by **1**/*i*PrOH is slower than that of L-LA (Table 1). Initial data showed that this reaction proceeds with slow initiation; this was confirmed by curve-fitting (SI Figure S11): $k_i = 1.70 \pm 0.04 \times 10^{-2}$ and $k_p = 3.05 \pm 0.06 \times 10^{-2} \text{ L}\cdot\text{mol}^{-1}\cdot\text{s}^{-1}$.

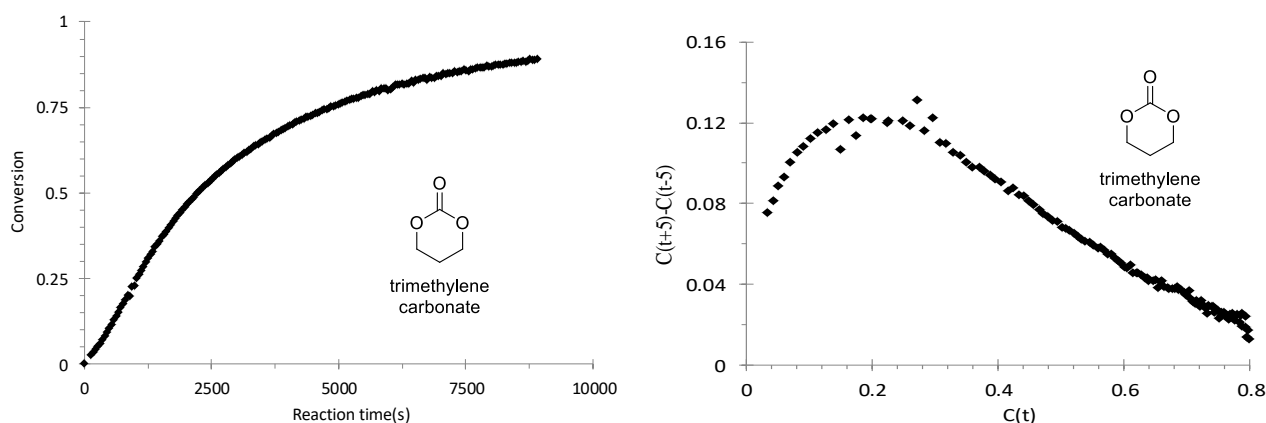


Figure 3. TMC polymerization catalyzed by **1**/*i*PrOH in toluene, 60 °C. $[\text{Sn}]_{\text{T}} = 10.0 \text{ mM}$, $[\text{TMC}]_{\text{T}} = 1.0 \text{ M}$, $[\text{TMC}]_{\text{T}}/[\text{Sn}]_{\text{T}}/[\textit{iPrOH}]_{\text{T}} = 100:1:10$. Left: Monomer conversion vs. reaction time. Right: Plot of the slope of conversion curve vs. conversion, showing the initiation phase.

Germanium catalysts. The germanium(II) complex $\{\text{LO}^3\}\text{Ge}(\text{N}(\text{SiMe}_3)_2)$ (**6**) has been shown to promote the ROP of L-LA.^{10g} The polymerization of L-LA (200 equiv) with this catalyst in the presence of 20 equiv of *i*PrOH ($[\text{L-LA}]_{\text{T}} = 1.00 \text{ M}$, $T = 70 \text{ }^\circ\text{C}$) allowed us to record a larger number of data points for conversions below 10%, and curve-fitting ($R^2 = 0.999$) demonstrated that propagation was faster than initiation (Figure S12; $k_i = 29.0 \pm 0.28 \times 10^{-4} \text{ L}\cdot\text{mol}^{-1}\cdot\text{s}^{-1}$, $k_p = 58.0 \pm 0.83 \times 10^{-4} \text{ L}\cdot\text{mol}^{-1}\cdot\text{s}^{-1}$).

3 Monomer depletion

During ROP reactions, the concentration of monomer decays with first-order dependence on monomer and catalyst concentration, that is

$$[\text{M}]_t = [\text{M}]_0 e^{-k_p [\text{Cat}]_{\text{T}} t}$$

Since the concentration in bound monomer is $[\text{M}]_{\text{B}} = [\text{M}]_0 - [\text{M}]_t$, the later phase of the polymerization can be fitted to eq (5):

$$[\text{M}]_{\text{B}} = [\text{M}]_0 (1 - e^{-k_p [\text{Cat}]_{\text{T}} t}) \quad (5)$$

The values of k_p determined using data points for conversion above 50% are in the range 1.12×10^{-2} to $48.00 \times 10^{-2} \text{ L}\cdot\text{mol}^{-1}\cdot\text{s}^{-1}$. These values are in excellent agreement with those estimated independently for the initial stage of the reaction using eq (4), which provides good confirmation of the validity of the non-linear model.

The monomer equilibrium concentration (0.014 M at $25 \text{ }^\circ\text{C}$, 0.024 M at $45 \text{ }^\circ\text{C}$ and 0.036 M at $60 \text{ }^\circ\text{C}$)^{9a} could be significant in our experiments carried out at relatively low monomer concentrations: $[\text{LA}]_T = 0.33 \text{ M}$ at $25 \text{ }^\circ\text{C}$, 0.5 M at $45 \text{ }^\circ\text{C}$ and 0.5 M at $60 \text{ }^\circ\text{C}$, where the maximum conversions are therefore 95.8, 95.1 and 92.9 %. The resulting asymptote at high conversion can be corrected by substituting $[\text{M}]_B$ by $[\text{M}]_B - [\text{M}]_{\text{eq}}$ as reported by Duchateau and co-workers,²¹ but we found that this had negligible effect on the calculated values of k_p .

4. Dependence of rate on [ROH] for tin(II)-mediated immortal ROP catalysis

In general, the rates of immortal lactide ring-opening polymerizations under steady-state conditions do not depend on $[\text{ROH}]_T$. However, with the present tin(II) systems, an increase in rate with increasing $[\text{ROH}]_T$ is observed for $[\text{ROH}]_T/[\text{Sn}]_T$ molar ratios in the range of 1:1 – 5:1. Figure 4 shows the effect of $[\text{ROH}]_T$, expressed as $[\text{polymer chains}]_T/[\text{Sn}]_T$ for constant $[\text{Sn}]_T = 10.0 \text{ mM}$, on the observed rate constant k_{obs} in the immortal ROP of L-LA catalyzed by **1** or **2** combined with *i*PrOH.

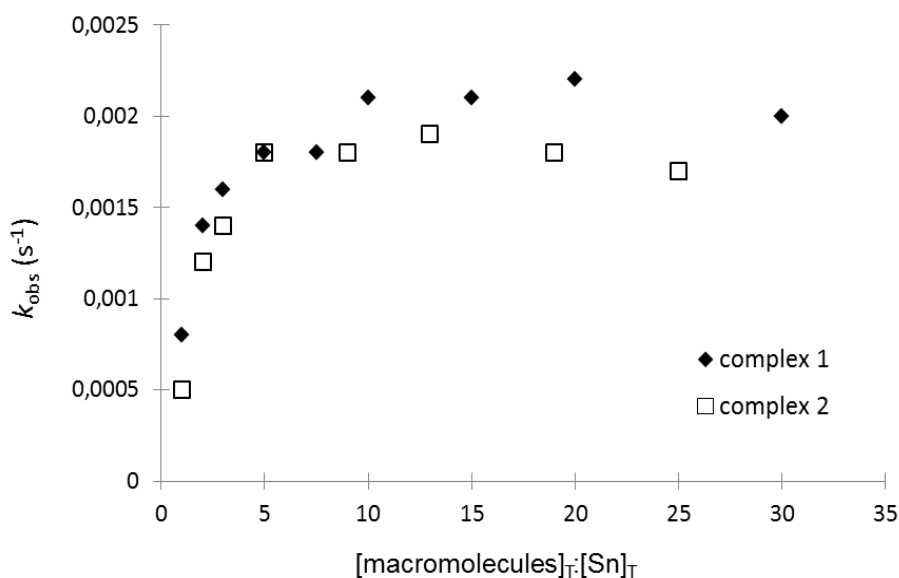


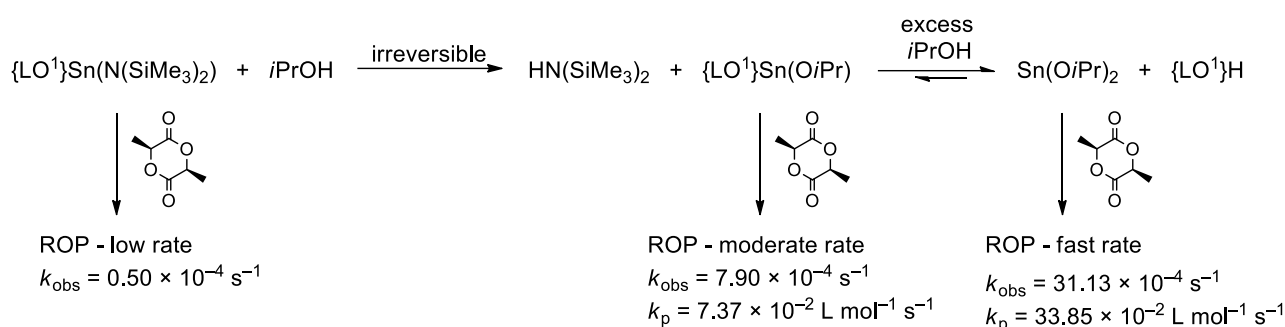
Figure 4. Dependence of the observed rate k_{obs} of L-LA polymerization catalyzed by the tin heteroleptic precatalysts **1** (◆) or **2** (□) on $[i\text{PrOH}]_{\text{T}}$ (expressed as $[\text{polymer chains}]_{\text{T}}/[\text{Sn}]_{\text{T}}$) in toluene- d_8 at 60 °C with $[\text{L-LA}]_{\text{T}} = 1.0 \text{ M}$, $[\text{Sn}]_{\text{T}} = 10.0 \text{ mM}$.

The lactato catalyst **2** is capable of polymerizing L-LA even without addition of *iPrOH* *via* insertion of the monomer in the Sn–O_{lactate} bond,^{11b} hence the total number of polymer chains generated *per* metal centre is equal to $1 + [i\text{PrOH}]_{\text{T}} / [\text{Sn}]_{\text{T}}$.²²

Significantly, the homoleptic tin *bis*(alkoxide) **3** ($n = 2$) shows different kinetic behavior (cf. SI Table S3). The addition of 0–24 equiv of *iPrOH* has no effect on the rate of reaction; within experimental error, the rates of polymerization with Sn(O*iPr*)₂ and {LO^{*i*}}Sn(O*iPr*) + *iPrOH* (4 equiv or more) are near-identical (and not retarded by added HN(SiMe₃)₂).

These kinetic data, together with the similarity of the propagation rates k_{p} determined using the kinetic model for the immortal ROP of L-LA with **1** or **5** in the presence of excess alcohol (Table 1), suggest that the increase in rate with increasing alcohol content observed for amido catalyst precursors is related to the generation of alkoxide species. The formation of {LO^{*i*}}Sn(O*iPr*) by reaction of {LO^{*i*}}Sn(N(SiMe₃)₂) with *iPrOH* is quantitative and irreversible, as demonstrated by NMR spectroscopy.²³ Moreover, we have shown previously that excess alcohol is able to reversibly release the phenol ligand from heteroleptic phenolate tin(II) alkoxide complexes.^{11a} Hence, further experiments were carried out to assess whether the increase in reaction rate with increasing [ROH]

is the result of the slow conversion of the poorly active tin amide precursor into the much more active alkoxide species $\{LO^i\}Sn(OiPr)$ and/or $Sn(OiPr)_2$ (Scheme 2). In this case, after formation of the isopropoxide(s), one would expect the reaction rate to be identical to that of the living polymerization, or that measured starting with pre-made $\{LO^i\}Sn(OiPr)$.



Scheme 2

Without added alcohol, the amido complexes **1**, **4** and **5** constitute sluggish ROP initiators, and do not afford controlled reactions.²⁴ For example, the batch-scale ROP of L-LA initiated by **5** in toluene took 4 h at 60 °C to yield near quantitatively a material of uncontrolled molecular weight ($[L-LA]_T/[Sn]_T = 25:1$, $[L-LA]_T = 0.75 \text{ M}$, $M_{n,\text{theo}} = 3,300 \text{ g} \cdot \text{mol}^{-1}$, $M_{n,\text{SEC}} = 59,600 \text{ g} \cdot \text{mol}^{-1}$, $M_w/M_n = 1.32$).

Table 2 summarises the influence of *i*PrOH concentration in the polymerization of L-LA catalyzed by **1–5** during NMR-scale reactions. Whereas the reaction catalyzed by **1** is slow in the absence of added alcohol (line 1), at the same temperature the reaction is faster and the molecular weight is controlled¹² if one equiv of *i*PrOH is added to the system (line 2). By contrast, the lactato complex **2** and the *bis*(isopropoxide) **3** both catalyze ROP of L-LA without alcohol (line 1). Rates increase in the sequence **1** < **2** < **3**. The addition of 2–10 equiv of $HN(SiMe_3)_2$ to **3** do not alter the rate of the polymerization catalyzed by tin *bis*(isopropoxide) (Table 2 lines 1, 5 and 12). Remarkably, the addition of 1 equiv of *i*PrOH or methyl (*S,S*)-lactidate to either **1** or **4** provides catalysts that essentially behave in the same fashion as **2** by itself (Table 2).

Table 2. Influence of *i*PrOH concentration in the polymerization of L-lactide catalyzed by **1–5**.^a

	[L-LA] _T /[Sn] _T /[ROH] _T	{LO ¹ }Sn(N(SiMe ₃) ₂) (1)		{LO ² }Sn(<i>t</i> Bu (<i>R</i>)-lactate) (2)		[Sn(O <i>i</i> Pr) ₂] ₂ (3)		{LO ⁴ }Sn(N(SiMe ₃) ₂) (4)		Sn(N(SiMe ₃) ₂) ₂ (5)	
		$k_{\text{obs}} \times 10^4$ (s ⁻¹)	$k_{\text{p}} \times 10^{2b}$ (L·mol ⁻¹ ·s ⁻¹)	$k_{\text{obs}} \times 10^4$ (s ⁻¹)	$k_{\text{p}} \times 10^{2b}$ (L·mol ⁻¹ ·s ⁻¹)	$k_{\text{obs}} \times 10^4$ (s ⁻¹)	$k_{\text{p}} \times 10^{2b}$ (L·mol ⁻¹ ·s ⁻¹)	$k_{\text{obs}} \times 10^4$ (s ⁻¹)	$k_{\text{p}} \times 10^{2b}$ (L·mol ⁻¹ ·s ⁻¹)	$k_{\text{obs}} \times 10^4$ (s ⁻¹)	$k_{\text{p}} \times 10^{2b}$ (L·mol ⁻¹ ·s ⁻¹)
1	100:1:0	0.50	<i>n/a</i> ^c	5.35	5.15 ± 0.01	31.13	33.85 ± 0.04			2.97	<i>n/a</i> ^c
2	100:1:1	7.90	7.37 ± 0.02	12.37	12.40 ± 0.01			3.57	3.50 ± 0.01	14.79	16.77 ± 0.06
3		5.47 ^d	5.22 ± 0.02 ^d								
4	100:1:2	14.05	13.83 ± 0.05	13.71	13.52 ± 0.02	27.79	32.23 ± 0.16	15.57	15.69 ± 0.01	14.51	15.39 ± 0.04
5						26.62 ^e	29.00 ± 0.10 ^e				
6	100:1:3	16.05	15.40 ± 0.09					16.51	17.31 ± 0.04		
7	100:1:4			18.11	17.49 ± 0.06	26.44	28.81 ± 0.10				
8	100:1:5	18.25	18.54 ± 0.05					19.25	19.97 ± 0.02		
9	100:1:7.5	23.28	22.17 ± 0.09								
10	100:1:8			18.44	18.87 ± 0.04	22.77	25.80 ± 0.16				
11	100:1:10	21.06	21.66 ± 0.05							18.62	17.49 ± 0.05
12						29.53 ^e	27.50 ± 0.20 ^e				
13	100:1:12			19.74	21.60 ± 0.16						
14	100:1:15	22.09	22.31 ± 0.08								
15	100:1:16					22.59	24.27 ± 0.09				
16	100:1:18			18.46	17.94 ± 0.03						
17	100:1:20	21.51	20.27 ± 0.10								
18	100:1:24			17.41	17.38 ± 0.04	21.44	22.50 ± 0.11				
19	100:1:30	20.19	18.41 ± 0.13								

^a Polymerization conditions: toluene-*d*₈, alcohol = *i*PrOH unless otherwise specified, [L-LA]_T = 1.0 M, [Sn]_T = 10 mM, and *T* = 60 °C. ^b Determined from

eq (5). ^c Data not suited to treatment with eq (5). ^d Exogenous transfer agent = methyl (*S,S*)-lactidate. ^e Exogenous transfer agent = HN(SiMe₃)₂.

Addition of more than 1 equiv of alcohol to **1–5** provides useful information. Instead of matching the catalytic activity observed for pre-formed *bis*(isopropoxide) **3**, the reactivity of the Sn(II) *bis*(amide) **5** does not change if two equiv of *i*PrOH are used instead of one. This suggests that, contrary to expectations, the *in situ* reaction **5** + 2 *i*PrOH does not generate tin *bis*(isopropoxide) but instead affords an intermediate species assumed to be Sn(O*i*Pr)(N(SiMe₃)₂) (as further evidenced by ¹¹⁹Sn NMR spectroscopy; *vide infra*). This mixed-ligand complex can be independently prepared by mixing **3** and **5** to give crystalline [Sn(μ -O*i*Pr){N(SiMe₃)₂}]₂ (**7**). ¹H DOSY NMR diffusion measurements showed that it remains dimeric in aromatic solution. The synthesis, crystal structure and spectroscopic data of **7** are given in the Supporting Information.

The complex engages in reversible equilibria leading to the formation of small amounts (*ca.* 3% at 25 °C, 9% at 60 °C) of [Sn(O*i*Pr)₂]₂ and Sn(N(SiMe₃)₂)₂. Increasing the temperature shifts the equilibrium towards homoleptic complexes; these changes are reversible on cooling to 25 °C. The ¹¹⁹Sn{¹H} NMR spectrum of isolated **7** exhibits a single triplet centred on $\delta_{119\text{Sn}} = +42.1$ ppm ($^1J_{119\text{Sn}-14\text{N}} = 263$ Hz). The product formed *in situ* by reaction of Sn(N(SiMe₃)₂)₂ (**5**) and 1 equiv of *i*PrOH in concentrations similar to those used for ROP reactions also featured the same resonance at $\delta_{119\text{Sn}} = +42.0$ ppm. On the other hand, three multiplets at $\delta_{119\text{Sn}} = +91.8$, $+35.4$ and $+4.0$ ppm were detected in the ¹¹⁹Sn{¹H} NMR spectrum of the reaction between **5** and 2 *i*PrOH. A spectrum also showing these resonances together with an additional one at $\delta_{119\text{Sn}} = +42.1$ ppm (corresponding to the formation of **7**) was also obtained by mixing **5** and 2 equiv of [Sn(O*i*Pr)₂]₂ (**3**). Attempts to establish clearly the origin of these resonances were unsuccessful, but they probably relate to bimetallic species of the type [Sn₂(O*i*Pr)(N(SiMe₃)₃)] and [Sn₂(O*i*Pr)₃(N(SiMe₃))], or even higher mixed tin(II) aggregates.

Complex **7** catalyzes ROP reactions without added alcohol. The Schlenk-scale ROP of L-LA at 60 °C initiated by **7** is controlled and gives 84% isolated yield after 4 h ([L-LA]_T/[Sn]_T = 25:1, [L-LA]_T = 0.75 M, $M_{n,\text{theo}} = 3,100$ g·mol⁻¹; $M_{n,\text{NMR}} = 4,500$ g·mol⁻¹; $M_{n,\text{SEC}} = 5,300$ g·mol⁻¹, $M_w/M_n = 1.17$). End-group analysis by ¹H NMR spectroscopy and MALDI-ToF MS shows that O*i*Pr is the

sole initiating group in ROP reactions catalyzed by **7**. During kinetically monitored polymerizations performed under identical conditions, the rate of reaction measured for **7** ($k_{\text{obs}} = 15.1 \pm 0.1 \times 10^{-4} \text{ s}^{-1}$ and $k_{\text{p}} = 15.7 \pm 0.1 \times 10^{-2} \text{ L}\cdot\text{mol}^{-1}\cdot\text{s}^{-1}$) matches that measured for **5/1–2** *i*PrOH (Table 2). $^{119}\text{Sn}\{^1\text{H}\}$ NMR spectroscopy proved informative on the speciation of the **5/1–2** *i*PrOH system.

Addition of 10 equiv of *i*PrOH to **5** ($\delta_{119\text{Sn}} = +776.0 \text{ ppm}$), *i.e.* under conditions pertaining to immortal ROP reactions, generates quantitatively the expected *bis*(isopropoxide) **3** (broad resonance at $\delta_{119\text{Sn}} = \text{ca. } -195 \text{ ppm}$), and indeed kinetic measurement for immortal polymerizations showed that **5** + 10 *i*PrOH ($k_{\text{obs}} = 18.7 \times 10^{-4} \text{ s}^{-1}$, $k_{\text{p}} = 17.49 \pm 0.05 \times 10^{-2} \text{ L}\cdot\text{mol}^{-1}\cdot\text{s}^{-1}$) catalyzed the reaction with rates very similar to **3** + 8 *i*PrOH ($k_{\text{obs}} = 22.7 \times 10^{-4} \text{ s}^{-1}$, $k_{\text{p}} = 25.86 \pm 0.16 \times 10^{-2} \text{ L}\cdot\text{mol}^{-1}\cdot\text{s}^{-1}$). Relevant $^{119}\text{Sn}\{^1\text{H}\}$ NMR data are given in the Supporting Information (Figure S15).

The above kinetic, synthetic and spectroscopic data and the previously demonstrated ability of excess *i*PrOH to displace phenolic ligands from aminoether-phenolate heteroleptic complexes $\{\text{LO}^i\}\text{Sn}(\text{OiPr})$ show that provided the alcohol concentration is sufficiently high – typically 7 equiv or more *vs.* Sn(II)– all catalyst precursors **1–5** generate the same active species, namely the homoleptic $\text{Sn}(\text{OiPr})_2$, at a rate which depends on the presence and nature of the ancillary phenolate ligand. All eventually polymerize L-LA at about the same rate under immortal conditions (Scheme 3 and Figure 5). Since initiation cannot be detected with **3** (the fastest catalyst), it appears reasonable to infer that the initiation observed in some cases for ROP reactions catalyzed by our tin(II) precatalysts in the presence of excess alcohol ($k_i < k_p$ in Table 1) results from slow formation of $\{\text{LO}^i\}\text{Sn}(\text{OiPr})$ and/or $\text{Sn}(\text{OiPr})_2$.²⁵ An identical phenomenon was observed by Duda and Penczek in their studies of ROP reactions (lactide, ϵ -caprolactone) catalyzed by the binary system $\text{Sn}(\text{2-ethyl-hexanoate})_2 + n\text{BuOH}$.^{9a-b} Although the mechanisms of formation of the active species were not investigated, these authors demonstrated that polymerization rates increased with $[n\text{BuOH}]_{\text{T}}$ until it reached a plateau for $[n\text{BuOH}]_{\text{T}}/[\text{Sn}]_{\text{T}} = 5\text{--}10$ and showed by MALDI-ToF mass spectrometry that several active species, namely (2-ethyl-hexanoate) $\text{Sn}(\text{OnBu})$, $\text{Sn}(\text{OnBu})_2$, and (2-

ethyl-hexanoate)SnOSn(*On*Bu), were all found in the reaction medium when excess *n*BuOH was used.

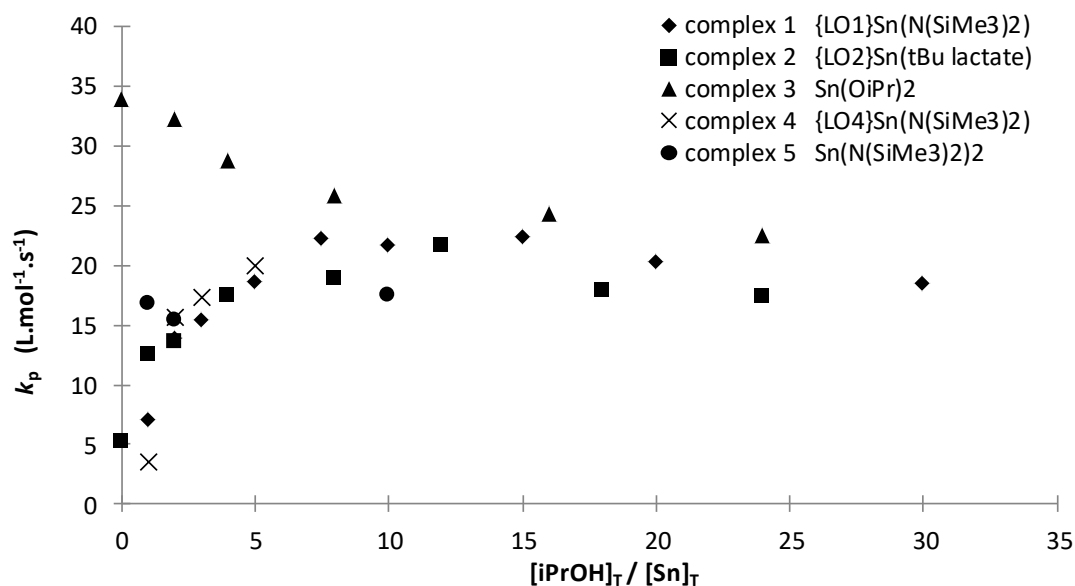
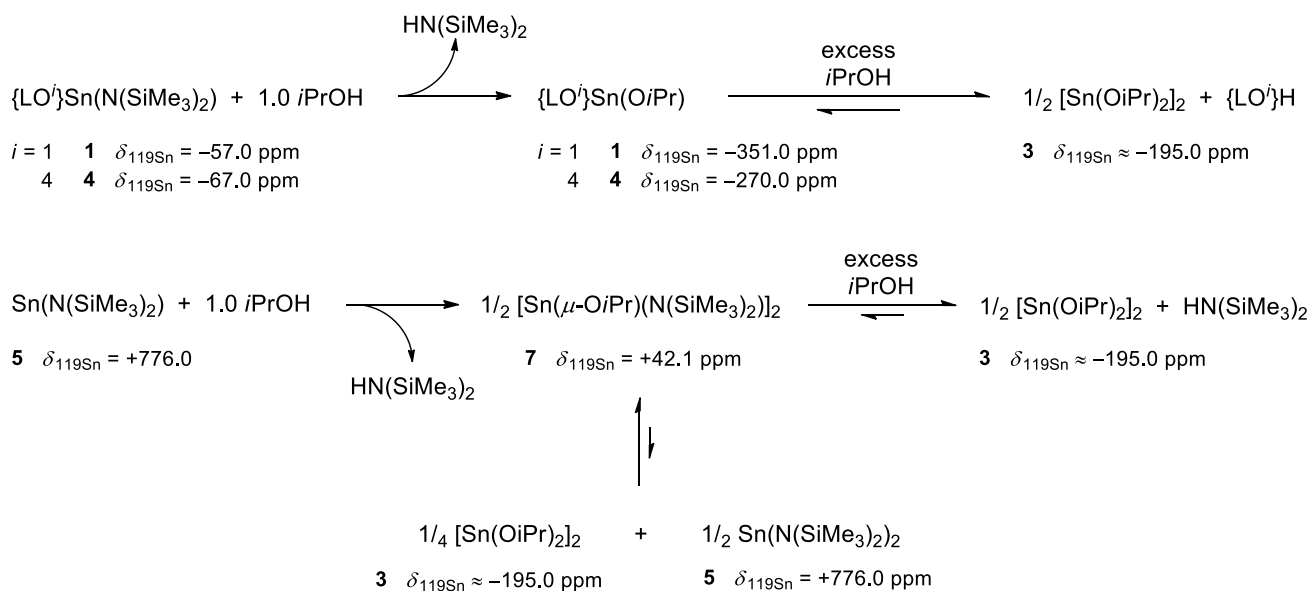


Figure 5. Variation of k_p with the ratio $[iPrOH]_T/[Sn]_T$ for the immortal ROP of L-lactide catalyzed by **1–5**. Polymerization in toluene- d_8 , $[Sn]_T = 10$ mM, $[L-LA]_T = 1.00$ M, and $T = 60$ °C.



Scheme 3.

Conclusion

A detailed kinetic analysis of the early stage of immortal ring-opening polymerization reactions catalyzed by a metal catalyst precursor and a chain transfer agent has been developed. Curve fitting to this kinetic scheme allows the extraction of initiation and propagation rate constants, k_i and k_p respectively. Systems showing the scenarios $k_i < k_p$, $k_i = k_p$ and $k_i > k_p$ have been identified. The results confirm that the rate of chain exchange under immortal conditions is much faster than propagation, but it is not directly accessible by this method. Future efforts are aimed at developing a model that can also describe the distribution of molecular weights and thus access lower estimates of k_e values. For a given catalytic system, the values of k_i (if it can be measured) and k_p can be extracted from a single experiment using the present kinetic treatment, whereas other methods require multiple experiments.^{2r,7,11a,13,26}

ROP catalysis mediated by group 14 complexes proceeds at a convenient rate to illustrate the model, comparing the values of k_p determined independently either using eq (4) or conventionally by steady-state methods, which are found to be in good agreement.

While the kinetic model enables the detection and quantification of an initiation period, it cannot provide direct evidence for the molecular process of initiation. There may be different reasons for the initiation phase observed for various catalysts (e.g. slow generation of a reactive metal-nucleophile species, catalyst aggregation, slow first monomer insertion...), but in all cases slow initiation points to mechanistic implications that need to be taken into account for a complete description of the immortal ROP process. In the present case of Sn(II) catalysts we propose that initiation is linked to the rate of generation of a mononuclear tin(II) alkoxide species in the presence of excess alcohol.

While tin(II) catalysts and L-lactide proved convenient to demonstrate its validity, the proposed kinetic model is of course general in nature and equally applicable to other substrates such as trimethylene carbonate and other catalysts. *In situ* FTIR techniques are able to record monomer conversion for systems that are too fast for conventional NMR techniques, and we are now planning

to implement these methods to the very active rare- and alkaline-earth ROP catalysts. The model proposed here will hopefully enable rapid and unambiguous comparisons of the efficiencies of ROP catalysts.

Our treatment relies only on general principles and includes the initiation stage of the reaction as a key part of the analysis. It comes as a complementary addition to the useful Michaelis-Menten-like kinetic treatment recently reported by Tolman and Hillmyer.¹³ The question of equilibria between aggregated and non-aggregated metal species remains. This will require additional investigations for a wider range of systems, but is of limited importance here since most *well-defined* ROP precatalysts (as opposed to $\text{Sn}^{\text{II}}(\text{2-ethyl-hexanoate})_2$) are known to produce monometallic active species under polymerization conditions,^{3,11,27} even when the precatalyst is dimeric in the solid-state or in solution.¹²

Specific features of tin(II)-mediated ROP catalysis have also become apparent. Reversible generation of tin(II) *bis*(alkoxide) has been demonstrated by $^{119}\text{Sn}\{^1\text{H}\}$ NMR studies when a small excess of alcohol is used with these tin(II) precatalysts, and this is consistent with the kinetic data recorded for $\{\text{LO}^i\}\text{Sn}(\text{N}(\text{SiMe}_3)_2)$, $\text{Sn}(\text{OiPr})_2$, $\text{Sn}(\text{OiPr})(\text{N}(\text{SiMe}_3)_2)$ and $\text{Sn}(\text{N}(\text{SiMe}_3)_2)_2$ in the presence of excess alcohol. Based on the present and our earlier study,^{11a} it is now established that with all these Sn(II) precatalysts, $\text{Sn}(\text{OiPr})_2$ and $\text{Sn}(\text{O-polymeryl})_2$ are the actual catalytically initiating and propagating species in immortal ROP reactions when a large excess of alcohol, typically 7 equiv or more, is employed.

Experimental Section

General procedures. All manipulations were performed under inert atmosphere using standard Schlenk techniques or in a glove-box. $\{\text{LO}^1\}\text{Sn}(\text{N}(\text{SiMe}_3)_2)$ (**1**),^{11a} $\{\text{LO}^2\}\text{Sn}(t\text{Bu}(R)\text{-lactate})$ (**2**),^{11b} $[\text{Sn}(\text{OiPr})_2]_2$ (**3**),¹² $\{\text{LO}^4\}\text{Sn}(\text{N}(\text{SiMe}_3)_2)$ (**4**),^{11b} $\text{Sn}(\text{N}(\text{SiMe}_3)_2)_2$ (**5**)²⁸ and $\{\text{LO}^1\}\text{Ge}(\text{N}(\text{SiMe}_3)_2)$ (**6**)^{10g} were prepared as reported. THF was distilled under argon from Na/benzophenone prior to use. Other solvents were collected from MBraun SPS-800 purification alumina columns. Deuterated

solvents were stored in sealed ampoules over activated 3 Å molecular sieves and degassed by several freeze-thaw cycles. L-LA (Total Petrochemicals) was purified by recrystallisation from a hot (80 °C) *i*PrOH solution, followed by two recrystallisations in hot (105 °C) toluene. TMC (Bohringer) was dissolved in THF, dried over CaH₂ and recrystallised from THF prior to use.

NMR spectra were recorded on Bruker AM-400 and AM-500 spectrometers. The probe temperature was regularly checked by standard methods relying on methanol (180–300 K) and ethylene glycol (300–380 K) solutions. All ¹H and ¹³C{¹H} chemical shifts were determined using residual signals of the deuterated solvents. ¹¹⁹Sn{¹H} NMR spectra were calibrated *vs.* SnMe₄.

Typical NMR-scale polymerization procedure. Immortal ROP reactions were systematically conducted in toluene-*d*₈. In a typical experiment, the catalyst and monomer were loaded in an NMR tube in the glove-box. The NMR tube was placed in a Schlenk flask, which was then removed from the glove-box and connected to the vacuum manifold. All subsequent operations were performed using Schlenk techniques. The appropriate amounts of solvent (toluene-*d*₈) and activator (*i*PrOH) were added to the NMR tube in this order at room temperature. The NMR tube was then sealed, briefly and very gently heated to ensure complete dissolution of the monomer and introduced in the spectrometer pre-set at the desired temperature (25, 45, 60, 70 or 100 °C). Time measurement started at this point. Data points were collected at regular intervals (typically 15–60 s), with a relaxation delay time sufficient to ensure accurate integration (D1 = 0.5 s) and NS = 8 scans until conversion of the monomer stopped (this usually coincided with near-full conversion). The conversion was reliably determined by integrating the methine region of PLLA (δ_{H} 5.00 ppm at 60 °C in toluene-*d*₈) *vs.* that of the monomer (δ_{H} 4.08 ppm at 60 °C in toluene-*d*₈). The accuracy of the measurements was corroborated by the good agreement between theoretical (based on the conversion, $M_{\text{n,theo}} = 144.13 \times [\text{L-LA}]_{\text{T}}/[\text{iPrOH}]_{\text{T}} \times \text{conversion}$) and experimental ($M_{\text{n,NMR}}$ determined by integration of the resonance of the methine hydrogens *vs.* that of the chain-ends) molecular weights. Reproducibility between identical runs was assessed under various conditions

and proved excellent; hence viscosity and potential mass transfer limitations have not been considered a potential source of error in kinetic measurements.

Typical Schlenk-scale polymerization procedure. In the glove-box, the metal catalyst (*ca.* 2.5–5.0 mg) was placed in a Schlenk flask together with the monomer (*ca.* 0.5–1.5 g). The Schlenk flask was sealed and removed from the glove box. All subsequent operations were carried out on a vacuum manifold using Schlenk techniques. The required amount of solvent (toluene) was added by syringe to the catalyst and the monomer, followed when required by addition of the activator (*i*PrOH, 3–10 μ L). The resulting mixture was immersed in an oil bath pre-set at the desired temperature (60 °C) and the polymerization time was measured from this point. Concentrations of L-lactide were in the range 1.0 – 2.0 M; complete dissolution was rapidly achieved upon vigorous stirring under the chosen experimental conditions. The reaction was terminated by addition of acidified MeOH (HCl, 1 wt-%) and the polymer was precipitated in methanol and washed thoroughly. The polymer was then dried to constant weight in a vacuum oven at 55 °C under dynamic vacuum ($< 5 \times 10^{-2}$ mbar).

Curve-fitting methods. Non-linear regressions using equation (4) were performed with the software DataFit 9.0. The concentration of enchaind monomer $[M]_B$ was calculated according to $[M]_B = [M]_T \times \text{conversion}$, using data points collected for conversion typically below 25%. Curve fittings were performed using a fixed value of k_e set at $100 \text{ L}\cdot\text{mol}^{-1}\cdot\text{s}^{-1}$. A time correction variable was introduced during the processing of curve-fitting experiment to stand for the time interval required by the reaction mixture in the NMR tube to reach temperature equilibration once inside the probe of the NMR spectrometer.

■ ASSOCIATED CONTENT

*SI Supporting Information

Details of the kinetic analysis; experimental and spectroscopic data on precatalyst **7**, data on polymer analysis. This material is available free of charge via the Internet at <http://pubs.acs.org>.

■ AUTHOR INFORMATION

Corresponding Author

*Tel: +33 223 233 019. E-mail: yann.sarazin@univ-rennes1.fr

Notes

The authors declare no competing financial interest.

■ ACKNOWLEDGMENTS

Assistance from Sourisak Sinbandhit ($^{119}\text{Sn}\{^1\text{H}\}$ NMR; *Centre Régional des Mesures Physiques de l'Ouest*, University of Rennes), Vincent Dorcet (X-ray diffraction crystallography, *Institut des Sciences Chimiques de Rennes*), Stephen Boyer (elemental analysis; London Metropolitan University), Jean-Paul Guégan (DOSY measurements; *Institut des Sciences Chimiques de Rennes*) and Total Petrochemicals (grant to V. P.) is gratefully acknowledged.

■ REFERENCES

-
- (a) Uhrich, K. E.; Cannizzaro, S. M.; Langer, R. S.; Shakesheff, K. M. *Chem. Rev.* **1999**, *99*, 3181. (b) Mecking, S. *Angew. Chem. Int. Ed.* **2004**, *43*, 1078. (c) *Handbook of Ring-Opening Polymerization*, Wiley-VCH, Eds: Dubois, P.; Coulembier, O.; Raquez, J.-M., Weinheim, **2009**. (d) *Poly(lactic acid): Synthesis, Structures, Properties, Processing and Applications*, John Wiley and Sons Inc., Eds: Auras, R.; Lim, L.-T.; Selke, S. E. M.; Tsuji, H., Hoboken, New Jersey, **2010**.
 - (a) Ovitt, T. M.; Coates, G. W. *J. Am. Chem. Soc.* **1999**, *121*, 4072. (b) Cheng, M.; Attygalle, A. B.; Lobkovsky, E. B.; Coates, G. W. *J. Am. Chem. Soc.* **1999**, *121*, 11583. (c) Chamberlain, B. M.; Cheng, M.; Moore, D. R.; Ovitt, T. M.; Lobkovsky, E. B.; Coates, G. W. *J. Am. Chem. Soc.* **2001**, *123*, 3229. (d) Ko, B.-T.; Lin, C.-C. *J. Am. Chem. Soc.* **2001**, *123*, 7973. (e) Ovitt, T. M.; Coates, G. W. *J. Am. Chem. Soc.* **2002**, *124*, 1316. (f) Nomura, N.;

-
- Ishii, R.; Akakura, M.; Aoi, K. *J. Am. Chem. Soc.* **2002**, *124*, 5938. (g) Williams, C. K.; Breyfogle, L. E.; Choi, S. K.; Nam, W.; Young Jr., V. G.; Hillmyer, M. A.; Tolman, W. B. *J. Am. Chem. Soc.* **2003**, *125*, 11350. (h) Cai, C.-X.; Amgoune, A.; Lehmann, C. W.; Carpentier, J.-F. *Chem. Commun.* **2004**, 330. (i) Majerska, K.; Duda, A. *J. Am. Chem. Soc.* **2004**, *126*, 1026. (j) Hormnirun, P.; Marshall, E. L.; Gibson, V. C.; White, A. J. P.; Williams, D. J. *J. Am. Chem. Soc.* **2004**, *126*, 2688. (k) Dove, A. P.; Gibson, V. C.; Marshall, E. L.; Rzepa, H. S.; White, A. J. P.; Williams, D. J. *J. Am. Chem. Soc.* **2006**, *128*, 9834. (l) Ma, H.; Spaniol, T. P.; Okuda, J. *Angew. Chem. Int. Ed.* **2006**, *45*, 7818. (m) Chmura, A. J.; Chuck, C. J.; Davidson, M. G.; Jones, M. D.; Lunn, M. D.; Bull, S. D.; Mahon, M. F. *Angew. Chem. Int. Ed.* **2007**, *46*, 2280. (n) Douglas, A. F.; Patrick, B. O.; Mehrkhodavandi, P. *Angew. Chem. Int. Ed.* **2008**, *47*, 2290. (o) Otero, A.; Fernández-Baeza, J.; Lara-Sánchez, A.; Alonso-Moreno, C.; Márquez-Segovia, I.; Sánchez-Barba, L. F.; Rodríguez, A. M. *Angew. Chem. Int. Ed.* **2009**, *48*, 2176. (p) N. Nomura, A. Akita, R. Ishii, M. Mizuno, *J. Am. Chem. Soc.* **2010**, *132*, 1750. (q) Pietrangelo, A.; Knight, S. C.; Gupta, A. K.; Yao, L. J.; Hillmyer, M. A.; Tolman, W. B. *J. Am. Chem. Soc.* **2010**, *132*, 11649. (r) Sarazin, Y.; Liu, B.; Roisnel, T.; Maron, L.; Carpentier, J.-F. *J. Am. Chem. Soc.* **2011**, *133*, 9069. (s) Bakewell, C.; Cao, T.-P.-A.; Long, N.; Le Goff, X. F.; Auffrant, A.; Williams, C. K. *J. Am. Chem. Soc.* **2012**, *134*, 20577.
- 3 (a) Dechy-Cabaret, O.; Martin-Vaca, B.; Bourissou, D. *Chem. Rev.* **2004**, *104*, 6147. (b) Williams, C. K.; Hillmyer, M. A. *Polym. Rev.* **2008**, *48*, 1. (c) Wheaton, C. A.; Hayes, P. G.; Ireland, B. J. *Dalton Trans.* **2009**, 4832. (d) Ajellal, N.; Carpentier, J.-F.; Guillaume, C.; Guillaume, S. M.; Hérou, M.; Poirier, V.; Sarazin, Y.; Trifonov, A. *Dalton Trans.* **2010**, *39*, 8363. (e) Thomas, C. M. *Chem. Soc. Rev.* **2010**, *39*, 165. (f) Stanford, M. J.; Dove, A. P. *Chem. Soc. Rev.* **2010**, *39*, 486. (g) Dijkstra, P. J.; Du, H.; Feijen, J. *Polym. Chem.* **2011**, *2*, 520. (h) Dagorne, S.; Normand, M.; Kirillov, E.; Carpentier, J.-F. *Coord. Chem. Rev.* **2013**, *257*, 1869. (i) Sauer, A.; Kapelski, A.; Fliedel, C.; Dagorne, S.; Kol, M.; Okuda J. *Dalton Trans.* **2013**, *42*, 9007.
- 4 (a) Asano, S.; Aida, T.; Inoue, S. *J. Chem. Soc., Chem. Commun.* **1985**, 1148. (b) Aida, T.; Inoue, S. *Acc. Chem. Res.* **1996**, *29*, 39.
- 5 In accordance with the common terminology used in the literature, the term “immortal” polymerization is employed here to designate controlled living ROP reactions performed in the presence of excess exogenous transfer agent such an alcohol (*i*PrOH in our case) or an amine, with fast and reversible exchange between active and dormant macromolecules; see for instance ref. 3d and 4.

-
- 6 (a) Liu, B.; Roisnel, T.; Maron, L.; Carpentier, J.-F.; Sarazin, Y. *Chem. Eur. J.* **2013**, *19*, 3986. (b) Clark, L.; Deacon, G. B.; Forsyth, C. M.; Junk, P. C.; Mountford, P.; Townley, J. P.; Wang J. *Dalton Trans.* **2013**, *42*, 9294.
- 7 For representative applications, see references 2d, 2r, 6 and: (a) Martin, E.; Dubois, P.; Jérôme, R. *Macromolecules* **2000**, *33*, 1530. (b) Liu, Y.-C.; Ko, B.-T.; Lin, C.-C. *Macromolecules* **2001**, *34*, 6196. (c) Shueh, M.-L.; Wang, Y.-S.; Huang, B.-H.; Kuo, C.-Y.; Lin, C.-C. *Macromolecules* **2004**, *37*, 5155. (d) Amgoune, A.; Thomas, C. M.; Carpentier, J.-F. *Macromol. Rapid Commun.* **2007**, *28*, 693. (e) Poirier, V.; Roisnel, T.; Carpentier, J.-F.; Sarazin, Y. *Dalton Trans.* **2009**, 9820. (f) Clark, L.; Cushion, M. G.; Dyer, H. E.; Schwarz, A. D.; Duchateau, R.; Mountford, P. *Chem. Commun.* **2010**, *46*, 273. (g) Zhao, W.; Cui, D.; Liu, X.; Chen, X. *Macromolecules* **2010**, *43*, 6678. (h) Hild, F.; Brelot, L.; Dagorne, S. *Organometallics* **2011**, *30*, 5457. (i) Cushion, M. G.; Mountford, P. *Chem. Commun.* **2011**, *47*, 2276. (j) Wang, Y.; Zhao, W.; Liu, X.; Cui, D.; Chen, E. Y.-X. *Macromolecules* **2012**, *45*, 6957. (k) Wang, Y.; Ma H. *Chem. Commun.* **2012**, *48*, 6729. (l) Li, G.; Lamberti, M.; Mazzeo, M.; Pappalardo, D.; Roviello, G.; Pellicchia, C. *Organometallics* **2012**, *31*, 1180. (m) Lamberti, M.; D'Auria, I.; Mazzeo, M.; Milione, S.; Bertolasi, V.; Pappalardo, D. *Organometallics* **2012**, *31*, 5551. (n) Liu, B.; Roisnel, T.; Guégan, J.-P.; Carpentier, J.-F.; Sarazin, Y. *Chem. Eur. J.* **2012**, *18*, 6289. (o) Zhao, W.; Wang, Y.; Liu, X.; Chen, X.; Cui, D. *Chem. Asian J.* **2012**, *7*, 2403. (p) Zhao, W.; Wang, Y.; Liu, X.; Cui, D. *Chem. Commun.* **2012**, *48*, 4483. (q) Zhao, W.; Wang, Y.; Liu, X.; Chen, X.; Cui, D.; Chen, E. Y.-X. *Chem. Commun.* **2012**, *48*, 6375. (r) Xu, C.; Yu, I.; Mehrkhodavandi, P. *Chem. Commun.* **2012**, *48*, 6806. (s) Li, C.-Y.; Wu, C.-R.; Liu, Y.-C.; Ko, B.-T. *Chem. Commun.* **2012**, *48*, 9628. (t) Hild, F.; Neehaul, N.; Bier, F.; Wirsum, M.; Gourlaouen, C.; Dagorne, S. *Organometallics* **2013**, *32*, 587.
- 8 See for instance: (a) Shan, J.; Haerkoenen, M.; Ropponen, J.; Harlin, A.; Heikkinen, H.; Raemoe, V.; Gaedda, T.; Nurmi, L.; Willberg-Keyriläinen, P. *PCT Int. Appl.* **2012**, WO 2012/160258. (b) Slawinski, M.; Hérou, M.; Wassenaar, J. *PCT Int. Appl.* **2013**, WO 2013/087812.
- 9 (a) Duda, A.; Penczek, S. *Macromolecules* **1990**, *23*, 1636. (b) Kowalski, A.; Duda, A.; Penczek, S. *Macromol. Rapid Commun.* **1998**, *19*, 567. (c) Kowalski, A.; Duda, A.; Penczek S. *Macromolecules* **2000**, *33*, 689. (d) Kricheldorf, H. R.; Kreiser-Saunders, I.; Stricker, A. *Macromolecules* **2000**, *33*, 702. (e) Kowalski, A.; Libiszowski, J.; Duda, A.; Penczek, S. *Macromolecules* **2000**, *33*, 1964. (f) Kowalski, A.; Duda, A.; Penczek, S., *Macromolecules* **2000**, *33*, 7359. (g) Penczek, S.; Duda, A.; Kowalski, A.; Libiszowski, J.; Majerska, K.; Biela,

-
- T. *Macromol. Symp.* **2000**, *157*, 61. (h) Biela, T.; Duda, A.; Penczek, S. *Macromol. Symp.* **2002**, *183*, 1. (i) Kowalski, A.; Libiszowski, J.; Biela, T.; Cypryk, M.; Duda, A.; Penczek, S. *Macromolecules* **2005**, *38*, 8170.
- 10 (a) Dove, A. P.; Gibson, V. C.; Marshall, E.L.; White, A. J. P.; Williams, D. J. *Chem. Commun.* **2001**, 283. (b) Aubrecht, K. B.; Hillmyer, M. A.; Tolman, W. B. *Macromolecules* **2002**, *35*, 644. (c) Nimitsiriwat, N.; Marshall, E. L.; Gibson, V. C.; Elsegood, M. R. J.; Dale, S. H. *J. Am. Chem. Soc.* **2004**, *126*, 13598. (d) Nimitsiriwat, N.; Gibson, V. C.; Marshall, E. L.; White, A. J. P.; Dale, S. H.; Elsegood, M. R. J. *Dalton Trans.* **2007**, 4464. (e) Nimitsiriwat, N.; Gibson, V. C.; Marshall, E. L.; Elsegood, M. R. J. *Inorg. Chem.* **2008**, *47*, 5417. (f) Nimitsiriwat, N.; Gibson, V.C.; Marshall, E. L.; Elsegood, M. R. J. *Dalton Trans.* **2009**, 3710. (g) Wang, L.; Roşca, S.-C.; Poirier, V.; Sinbandhit, S.; Dorcet, V.; Roisnel, T.; Carpentier, J.-F.; Sarazin Y. *Dalton Trans.* **2014**, *43*, 4268.
- 11 (a) Poirier, V.; Roisnel, T.; Sinbandhit, S.; Bochmann, M.; Carpentier, J.-F.; Sarazin, Y. *Chem. Eur. J.* **2012**, *18*, 2998. (b) Wang, L.; Kefalidis, C. E.; Sinbandhit, S.; Dorcet, V.; Carpentier, J.-F.; Maron, L.; Sarazin, Y. *Chem. Eur. J.* **2013**, *19*, 13463.
- 12 Wang, L.; Bochmann, M.; Cannon, R. D.; Carpentier, J.-F.; Roisnel, T.; Sarazin, Y. *Eur. J. Inorg. Chem.* **2013**, 5896.
- 13 (a) Ding, K.; Miranda, M. O.; Moscato-Goodpaster, B.; Ajellal, N.; Breyfogle, L. E.; Hermes, E. D.; Schaller, C. P.; Roe, S. E.; Cramer, C. J.; Hillmyer, M. A.; Tolman, W. B. *Macromolecules* **2012**, *45*, 5387. (b) Miranda, M. O.; DePorre, Y.; Vazquez-Lima, H.; Johnson, M. A.; Marell, D. J.; Cramer, C. J.; Tolman, W. B. *Inorg. Chem.* **2013**, *52*, 13692.
- 14 For reviews, see: (a) Bochmann, M. *J. Organomet. Chem.* **2004**, *689*, 3982. (b) M. Bochmann, *Organometallics* **2010**, *29*, 4711. See also: (c) Liu, Z.; Somsook, E.; Landis, C. R. *J. Am. Chem. Soc.* **2001**, *123*, 2915. (d) Liu, Z.; Somsook, E.; White, C. B.; Rosaaen, K. A.; Landis, C. R. *J. Am. Chem. Soc.* **2001**, *123*, 11193. (e) Sillars, D. R.; Landis, C. R. *J. Am. Chem. Soc.* **2003**, *125*, 9894. (f) Song, F.; Cannon, R. D.; Lancaster, S. J.; Bochmann, M. *J. Mol. Catal.* **2004**, *218*, 21.
- 15 Note that in Carother's theory for step-growth polymerizations, the reactivity of functional groups is independent of the molecule size. See: *Principles of Polymerization, Fourth Edition*; G. Odian, John Wiley and Sons Inc., Hoboken, New Jersey, **2004**.
- 16 Zinc, alkaline- and rare-earth precatalysts are too fast for kinetic monitoring by ¹H NMR, while Li- and Al-based ones are too slow. See for instance references 7d-f and 7n.
- 17 If this value was not set initially, *i.e.* when k_e was allowed to refine freely, the different software that we used (Origin, Matlab or DataFit) did not converge to a single solution.

-
- 18 Changing k_e by 12 orders of magnitude had only marginal influence on the resulting values of k_p and k_i . For ROP of L-LA catalyzed by **1**/*i*PrOH at 25 °C with $[L-LA]_T/[1]_T/[iPrOH]_T = 66:1:5$ (corresponding to entry 1 in Table 1), when k_e is deliberately fixed at values between 10^{-6} to 10^6 L·mol⁻¹·s⁻¹, k_p and k_i only vary from 1.09×10^{-2} to 1.85×10^{-2} L·mol⁻¹·s⁻¹ and 3.73×10^{-3} to 6.17×10^{-3} L·mol⁻¹·s⁻¹ respectively, *i.e.* the observed variations are kinetically insignificant. Similar results were observed when the value of k_e was tuned in the same manner for all other experiments taken from Table 1.
- 19 Polymerization conditions were similar to those for entries 12–13 in Table 1: T = 60 °C, [L-LA]₀ = 1.0 M, [Sn]_T = 2.50–50.0 mM. The intersection with the concentration axis was very close to zero, suggesting that minimal catalyst deactivation occurred through the presence of impurities. Details are available from the Supporting Information and ref. 12.
- 20 Under the experimental conditions of Table 1, the homoleptic *bis*(alkoxide) **3** generally proved much too fast to record data points in the early stage of the polymerization, which argues against the occurrence of a slow initiation step.
- 21 Pepels, M. P. F.; Bouyahyi, M.; Heise, A.; Duchateau, R. *Macromolecules* **2013**, *46*, 4324.
- 22 For a given catalyst precursor, one can generally define [polymer chains]_T = $n \times [Sn]_T + [iPrOH]_T$, where n is the number of alkoxide group found in the initial complex: for **1**, $n = 0$; for **2**, $n = 1$.
- 23 Both ¹H and ¹¹⁹Sn{¹H} NMR spectroscopies show unequivocally the irreversible release of free HN(SiMe₃)₂ upon reaction of {LO^{*i*}}Sn(N(SiMe₃)₂) and *i*PrOH; see ref. 11 and present work. Also, kinetic data in Table 2 show that (*i*) Sn(N(SiMe₃)₂) is a very slow ROP initiator compared to Sn(O*i*Pr)₂, and (*ii*) the addition of 2–10 equiv of HN(SiMe₃)₂ to Sn(O*i*Pr)₂ does not affect the rate of the living ROP of L-LA catalyzed by the latter compound.
- 24 Similar observations have already been made before for other complexes, for instance by Gibson (ref. 10d) or by Tolman and Hillmyer: Aubrecht, K. B.; Chang, K.; Hillmyer, M. A.; Tolman, W. B. *J. Polym. Sci., Polym. Chem.* **2001**, *39*, 284.
- 25 It is in fact very likely that with these systems, the rate of initiation is directly related to the rate of formation of the reactive species. Several attempts to demonstrate this point by measuring the rate of formation of the tin(II)-alkoxide species under conditions related to ROP reactions have been made but failed due to experimental constraints.
- 26 Silvernail, C. M.; Yao, L. J.; Hill, L. M. R.; Hillmyer, M. A.; Tolman, W. B. *Inorg. Chem.* **2007**, *46*, 6565.

- 27 (a) Chisholm, M. H.; Choojun, K.; Chow, A. S.; Fraenkel G. *Angew. Chem. Int. Ed.* **2013**, *52*, 3264. (b) Balasanthiran, V.; Chisholm, M. H.; Choojun, K.; Durr, C. B. *Dalton Trans.* **2014**, 43, 2781.
- 28 Schaeffer, C. D.; Zuckerman, J. J. *J. Am. Chem. Soc.* **1974**, *96*, 7160.

For the Table of Contents only:

